Experimental Determination of Concentration-Dependent Carbon Dioxide Diffusivity in LDPE

J. Tendulkar, S. R. Upreti, A. Lohi

Department of Chemical Engineering, Ryerson University, Toronto M5B 2K3, Canada

Received 28 November 2007; accepted 21 July 2008
DOI 10.1002/app.29059
Published online 3 October 2008 in Wiley InterScience (www.interscience.wiley.com).

ABSTRACT: In this work, we experimentally determine the concentration-dependent diffusivity of carbon dioxide in low-density poly(ethylene) (LDPE). For this purpose, experiments are carried out to obtain pressure-decay data for isothermal diffusion of the gas in the polymer. Based on a detailed mass transfer model, variational calculus is used to establish the conditions necessary to yield the concentration-dependent diffusivity that enables the model-predicted mass of absorbed gas in polymer to match with the experimental counterpart. A computational algorithm is implemented to solve the model and the conditions and obtain the diffusivities. Determined at 120 and 130°C for four different pressures in the range 0.352 to 1.232 MPa, the diffusivities are strong unimodal functions of gas concentration in polymer and of the order 10^{-9} m^2 s^{-1}. Mathematical correlations are developed to calculate the diffusivity at a given temperature, pressure, and gas concentration. © 2008 Wiley Periodicals, Inc. J Appl Polym Sci 111: 380–387, 2009

Key words: carbon dioxide; polyethylene; experimental diffusivity; concentration dependence; variational calculus

INTRODUCTION

Gas diffusion in polymers is of significant importance in several applications such as polymerization, monomer recycling, stripping, drying, coating, foaming, and polymer purification. Depending on diffusion, the rates at which chemical species are added to or removed from polymers impart important physical and chemical properties to the polymer products. It may be noted that diffusion in many polymer systems takes place under extreme temperature and pressure conditions and exhibits a strong dependence on concentration. These thermodynamically nonideal systems comprise concentrated solutions of polymers and chemical species as opposed to very dilute regimes where theoretical advancements have been most significant. The improved design and optimization of the polymer systems, and especially polymer purification processes require experimental concentration-dependent diffusivity data, which are scarce at present.

Diffusivity is a coefficient in Fick's first law, which results from the statistical modeling of a large nonequilibrium system.[1] This coefficient is a product of the true transport property called Maxwell-Stefan diffusivity,[2] and a thermodynamic nonideality factor related to the concentration of a chemical species in the medium. Hence, diffusivity (Fickian) is a function of the species concentration at a given temperature and pressure. Depending upon the nonideality, the diffusivity of a species varies with its concentration in the medium, with the effect being significant at finite concentrations, and notably present in gas–polymer systems. Only some of them[3–7] have been experimentally investigated in the past, but using simplified mass transfer models and (or) assuming negligible effects of the nonideality.

In this work, our objective is to determine the diffusivity of gas as a function of its concentration in polymer and capture the nonideal effects. To that end, we employ a rigorous mass transfer model and the noninvasive experimental method of pressure decay.[8–11] In this method, pressure versus time data during gas diffusion in a dense phase (such as liquid, polymer, and heavy oil) are generated for use in the determination of diffusivity subject to the model of the experimental mass transfer process. The experimentation has been rendered very effective and reliable by Koros and Paul,[12] who introduced an auxiliary cell to startup the experiment with a known quantity of conditioned gas mass. Thus, we follow the authors' approach in conjunction with a distributed parameter mass transfer model and functional optimization. The

Correspondence to: S. R. Upreti (supreti@ryerson.ca).
Contract grant sponsors: Canada Foundation of Innovation, Ontario Innovation Trust, Natural Sciences and Engineering Research Council (NSERC) of Canada, Department of Chemical Engineering, Ryerson University.

concentration-dependent gas diffusivity of carbon dioxide is determined in low-density poly(ethylene) (LDPE) at 120 and 130°C for four different pressures in the range 0.352–1.232 MPa.

The unique feature of this work is that it allows the natural evolution of diffusivity versus concentration function in agreement with experimental data and subject to the detailed mathematical model. Since no particular form of the diffusivity function is presumed, the diffusivity results are optimal to the maximum degree. They are not influenced or limited by any postulated or preconceived functional form. As a result, they effectively delineate the nonideal behavior of gas diffusivity at finite concentrations in the polymer.

EXPERIMENTAL SETUP

Figure 1 shows the schematic of the experimental setup. The primary component is a cylindrical pressure cell with a concentric 3.7-cm diameter cylindrical slot at the bottom to hold a polymer sample. The lid of the cell has a glass window allowing a complete view of the polymer surface to an external online Keyence® (Keyence Canada Inc., Ontario, Canada) LKG displacement laser sensor, which tracks the polymer surface movement with 10 μm accuracy. The lid is screwed to the cell and sealed using a Teflon core composite Viton O-ring. As shown in the figure, the cell is connected to a gasholder through valves A and B and a preheating coil. The gasholder is a high-pressure gas capsule for storing and preconditioning the gas obtained from an external gas tank. An online Paroscientific Digiquartz® (Paroscientific Inc., Redmond, WA) Intelligent pressure transmitter is provided between valves A and B to gather pressure versus time data. It has a resolution of ±6 Pa, which is achieved by its quartz crystal resonator whose frequency of oscillation varies with pressure-induced stress. A vacuum port is also provided to the cell through valve C.

As outlined in Figure 1, the cell and the gasholder are placed inside a forced convection oven with a temperature control capability of ±0.5°C. Mounted outside the oven, the pressure transmitter and the laser sensor are connected to a computer data acquisition system. The oven along with instruments is mounted on an air table, which absorbs any vibrations from the surroundings. During an experiment, the cell and the piping between valves A and C form a closed isothermal system for pressure decay as the gas diffuses into the polymer phase.

Experimental procedure

Before each experiment, the closed isothermal system was tested for leaks by pressurizing it to 1.25 times the experimental pressure for 12 h at the experimental temperature. Valves A and C were closed while valve B was open during the testing. After it was successful, valve C was opened, and LDPE granules were placed in the sample slot to melt under vacuum at the experimental temperature and form a cylindrical layer of uniform thickness. Having thus prepared the LDPE sample, valve A was opened after closing valve B. The setup inside the oven was conditioned by maintaining it at the experimental temperature under 4 mmHg vacuum for 8 h. During this time, the pressure cell was finally checked for any leaks. The laser sensor was then positioned and calibrated to track the distance from the polymer surface.

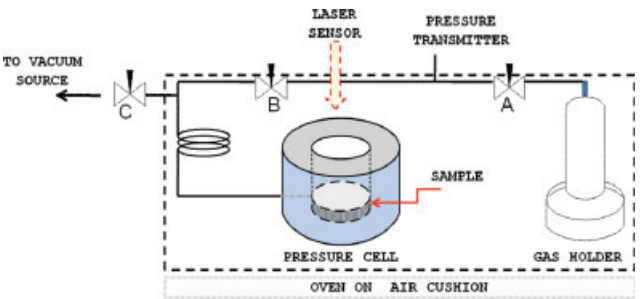

Figure 1 Schematic diagram of the experimental setup. [Color figure can be viewed in the online issue, which is available at www.interscience.wiley.com.]

The experiment was started by quickly introducing the gas above and parallel to the polymer surface inside the cell. This step was accomplished by simultaneously opening valve B and closing valve A to isolate the cell from the gasholder. As the introduced gas absorbed in the polymer phase, the system pressure decayed with time. The readings of the pressure transmitter and the laser sensor were recorded every 1.2 s until the time no pressure reduction was detectable. That is the time when the mass fraction of the gas in the polymer sample tends to a uniform equilibrium value. The experiment at that time was terminated, and valve C was gradually opened to release the gas. The polymer slot was cleaned up for the next experiment. Figure 2 shows a typical set of pressure versus time data obtained from experiments.

The polymer used in the experiments was an LDPE resin contributed by Nova Chemicals (Nova Chemicals Corporation, Sarnia, Ontario, Canada). The resin typically has 12,100 kg $kmol^{-1}$ number-average molecular weight, 7.36 polydispersity, and the third moment of molecular weight distribution of 286,000. The gas used in the experiments was 99% pure carbon dioxide supplied from British Oxygen (British Oxygen Corporation Canada Ltd., Ontario, Canada).

THEORETICAL DEVELOPMENT

Because the polymer is not volatile, the recorded pressure versus time data, the pressure–volume–

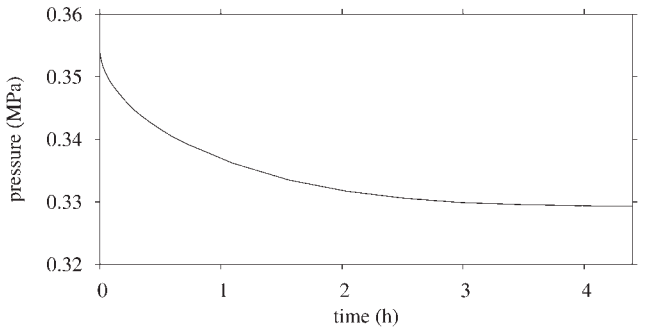

Figure 2 Pressure versus time data for an experiment at 130°C.

temperature relationship of the gas, and the volume change data for the gas–polymer mixture yield, the experimental mass of gas absorbed in the polymer at any time. The primary objective is to determine the diffusivity (D) of a gas as a function of its mass concentration (ω) in the polymer phase. The criterion for the determination is the agreement of the experimental mass of the gas absorbed in the polymer with that predicted by the mass transfer model, which has the concentration-dependent diffusivity as an optimization parameter.[13]

Mass transfer model

The polymer is homogenous with no gas in the beginning. During the experimental process, the transfer of gas to the polymer is solely due to molecular diffusion along z-direction perpendicular to the top polymer surface exposed to the gas. Furthermore, the transfer is a pure physical phenomenon since carbon dioxide is nonreactive with LDPE under the experimental temperature and pressure conditions. With these assumptions, the mass balance of the gas in the polymer is given by

$$\frac{\partial \omega}{\partial t} = -\left[\frac{\partial N}{\partial z}\right] \tag{1}$$

where N is the mass flux of the gas related to its diffusive flux,

$$j = -D\frac{\partial \omega}{\partial z} \tag{2}$$

and the bulk flux ($N_b = N$) as follows:

$$N = wN_b + j = wN + j \tag{3}$$

In the above equation, w is the mass fraction of gas in the polymer. In the aforementioned experiments, the laser sensor of 10 μm least count did not detect any swelling of polymer samples. This fact implies that the volume change of mixing is negligible. Thus,

$$w = \frac{\omega V_{\mathrm{gp}}}{\omega V_{\mathrm{gp}} + \rho_p V_p} = \frac{\omega V_{\mathrm{gp}}}{\omega V_{\mathrm{gp}} + \rho_{\mathrm{p}} V_{\mathrm{gp}}} = \frac{\omega}{\omega + \rho_p} \tag{4}$$

where ρ_p is the density of pure polymer having a volume V_p before penetration by the gas, which forms a gas–polymer mixture of volume, V_{gp}. Equations (2)–(4) give

$$N = \frac{D}{1-w}\frac{\partial \omega}{\partial z} \tag{5}$$

which when substituted in eq. (1) yields the final form of continuity equation

$$\frac{\partial \omega}{\partial t} = D\left[1 + \frac{\omega}{\rho_p}\right]\frac{\partial^2 \omega}{\partial z^2} + \left[\left(1 + \frac{\omega}{\rho_p}\right)\frac{\partial D}{\partial \omega} + \frac{D}{\rho_p}\right]\left(\frac{\partial \omega}{\partial z}\right)^2 \equiv f \tag{6}$$

where $\omega = \omega(z, t)$ is the mass concentration of the gas in the polymer at a depth z and a time t. A similar form of continuity equation has been derived by one of the authors for gas–bitumen systems.[13] The diffusivity D depends on ω so that it is the composite function, $D = D[\omega(z, t)]$. Since there is no gas in the polymer at $t = 0$,

$$\omega(z, 0) = 0; \quad 0 < z \leq L \tag{7}$$

The interfacial gas concentration is known at all times, i.e.,

$$\omega(0, t) = \omega_{\mathrm{sat}}(t); \quad 0 \leq t \leq T \tag{8}$$

where T is the final time. Because there is no mass transfer at the bottom of the cell,

$$\left.\frac{\partial \omega}{\partial z}\right|_{z=L} = 0; \quad 0 \leq t \leq T \tag{9}$$

Equations (7)–(9) are the initial and boundary conditions for eq. (6).

The objective

Mathematically, the objective functional can be written as

$$\min_{I} = \int_0^T \left[m_{\mathrm{gp},m}(t) - m_{\mathrm{gp},e}(t)\right]^2 dt \tag{10}$$

At any time t, $m_{\mathrm{gp},e}$ is the experimental mass of gas absorbed in the polymer, whereas $m_{\mathrm{gp},m}$ is the model-predicted gas mass absorbed in polymer given by

$$m_{\mathrm{gp},m}(t) = \int_0^L \omega(z, t) A dz \tag{11}$$

In the above equation, L is the depth of the polymer phase having a cross-sectional area A. Note that $\omega(z,t)$ is given by highly nonlinear partial differential

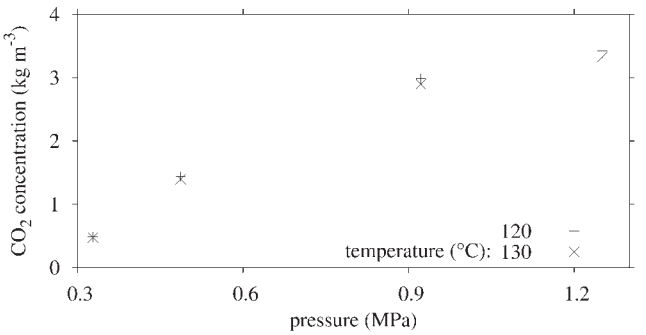

Figure 3 Saturation mass concentration of carbon dioxide in the LDPE under experimental conditions.

equation, eq. (6), having $D(\omega)$ as the optimization or control function. As shown in Appendix, the necessary condition for the constrained minimum of I is

$$J = \lambda \frac{\partial f}{\partial D} = 0; \quad 0 \le z \le L; \quad 0 \le t \le T \tag{12}$$

subject to the satisfaction of eq. (6) as well as the equation for the adjoint variable, $\lambda(z, t)$, given by

$$\frac{\partial \lambda}{\partial t} = 2A(m_{\mathrm{gp,mod}} - m_{\mathrm{gp},e}) + \frac{\lambda}{\rho_p}\frac{\partial D}{\partial \omega}\left(\frac{\partial \omega}{\partial z}\right)^2 + \left(1 + \frac{\omega}{\rho_p}\right) \times \left[\lambda \frac{\partial D}{\partial \omega}\frac{\partial^2 \omega}{\partial z^2} + \lambda \frac{\partial^2 D}{\partial \omega^2}\left(\frac{\partial \omega}{\partial z}\right)^2 - D\frac{\partial^2 \lambda}{\partial z^2}\right] \tag{13}$$

The above equation has the initial condition,

$$\lambda(z, T) = 0; \quad 0 < z \le L \tag{14}$$

and the two boundary conditions,

$$\lambda(L, t) = 0; \quad 0 \le t \le T \tag{15}$$

$$\lambda(0, t) = 0; \quad 0 \le t \le T \tag{16}$$

Diffusivity calculation

The diffusivity was calculated by integrating eq. (6) with an initial guessed diffusivity and storing the results for use in the backward integration of eq. (13). This exercise enabled the calculation of J [from eq. (12)], which was used to apply gradient corrections to the diffusivity. This functional optimization procedure was repeated until there was no further reduction in I. Note that the calculation of I requires $m_{\mathrm{gp},e}$, which was obtained from the experimental pressure versus time data in conjunction with the PVT relationship of the gas.[14]

The value of $m_{\mathrm{gp},e}$ at the final pressure corresponding to an infinite time yields the saturation mass concentration of the gas, i.e., $\omega_{\mathrm{sat}}[P(t)]$, which furnishes the boundary condition expressed by eq. (8). $\omega_{\mathrm{sat}}(P)$ was determined at the two experimental temperatures by performing 10 experiments for extended time durations. Its values are provided in Figure 3. It is observed that the solubility of carbon dioxide in the LDPE resin at a given temperature increases with pressure but decreases with temperature as is the trend reported elsewhere.[8]

Equations (6) and (13) were numerically integrated after applying second-order finite difference formulas along z direction. The time period for the integrations was carefully selected to restrict pressure decay to less than 2% of the initial pressure. The fifth-order adaptive step method of Runge-Kutta-Fehlberg was employed with Cash-Karp parameters.[15] Diffusivity was implemented as a smooth cubic spline interpolated function, $D(\omega)$, over specified gas mass concentrations between zero and the maximum (at time $t = 0$). For best results, as several numerical experiments had indicated, $D(\omega)$ was initialized to a uniform value as high as possible without causing $m_{\mathrm{gp},m}(t)$ to cross $m_{\mathrm{gp},e}(t)$.

During the computations, cubic splines were used to interpolate the following: $D(\omega)$ as well as its first and second derivatives with respect to ω, $m_{\mathrm{gp},e}(t)$, $\omega_{\mathrm{sat}}[P(t)]$, $\omega(t)$ at a given z, and the variational derivative $J(\omega)$ derived in Appendix. The values of $J(\omega)$ were time-averaged before their usage for the gradient correction in $D(\omega)$ by Broyden-Fletcher-Goldfarb-Shanno algorithm.[15] The maximum correction in diffusivity was limited to 1% of its value to allow slow but steady approach to the minimum. Table I provides the parameters used in the calculations. The number of grid points and diffusivity values and the accuracy of integrations were determined after varying those parameters to the point when the changes in the solution became insignificant.

Figure 4 shows the convergence of the functional optimization procedure yielding the optimal $D(\omega)$. With the iterative refinement in the initial $D(\omega)$, the value of I decreases monotonically to a low value of 1.6×10^{-11}, that is, the optimal point when the gradient corrections of eq. (7) tend to zero and further improvement becomes insignificant. The experimental and the optimally calculated values of the gas mass in polymer agree well as shown in the figure.

TABLE I
Parameters Used in Diffusivity Calculations

Parameter	Value
Mass of polymer	6×10^{-3} kg
Diameter of polymer sample holder	3.7×10^{-2} m
Volume of the gas phase in the pressure cell	15.6337×10^{-6}
Initial guess for D	8×10^{-10} m^2 s^{-1}
No. of D vs. ω points	75
No. of grid points along the sample depth	60

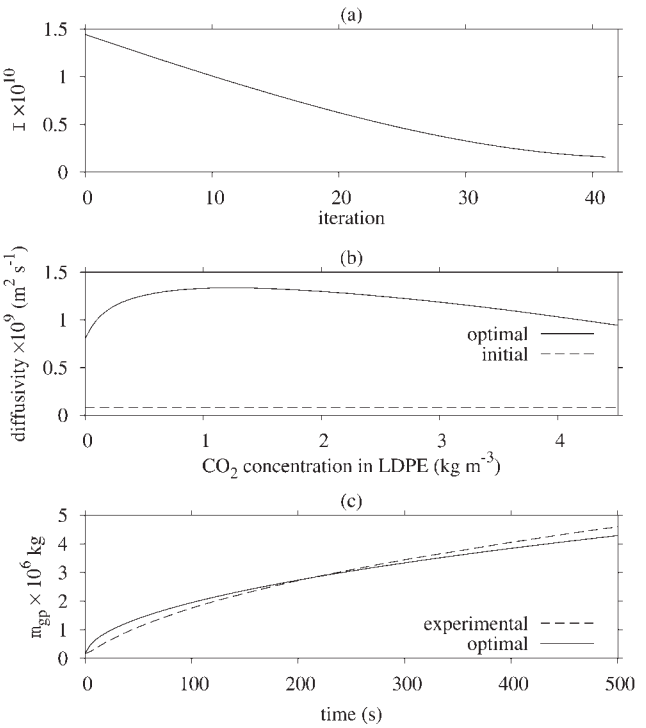

Figure 4 (a) The convergence of I to the optimum resulting in (b) the optimal $D(\omega)$, and (c) the match between the corresponding $m_{gp,m}(t)$ and $m_{gp,e}(t)$.

RESULTS AND DISCUSSION

Using the aforementioned functional optimization procedure, diffusivity versus mass concentration results were obtained at 120 and 130°C for four different pressures in the range 0.352 to 1.232 MPa in the carbon dioxide–LDPE system. Presented in Figure 5, those results showed that with the gas mass concentration, the diffusivity increases until it attains a maximum value before decreasing to lower values. The maximum diffusivity is 1.35–13 times the minimum, thereby indicating the strong concentration dependence of the gas diffusivity. As is typical for many hydrocarbon systems, the diffusivities are generally of the order 10^{-9} m^2 s^{-1}. Their peak values lie between 9.77×10^{-10} and 3.05×10^{-9} m^2 s^{-1}.

Since higher pressure enhances the driving force for gas absorption, the domain of diffusivity function (i.e., the interval zero-maximum gas mass concentration) increases with pressure at a given temperature. As seen in the figures, the diffusivity profiles span more to the right at a higher pressure. At a given gas mass concentration and pressure, the diffusivity is slightly higher for the higher temperature. However, the relationship of diffusivity with pressure is not that straightforward as is observed from the figure. At a given gas concentration, a higher pressure increases the frequency of intermolecular collisions but reduces the intermolecular distances. Although the first effect of increased collision frequency facilitates gas diffusion, the second opposing effect of reduced intermolecular distances impedes it. Thus, depending on the gas mass concentration, the diffusivity increases or decreases with pressure if the first or second effect dominates. The first effect is generally observed to dominate at a higher value of gas mass concentration, and over a larger part of its interval. As a result, the gas mass concentration-averaged gas diffusivity increases with pressure in addition to increasing with temperature.

Table II shows the concentration-averaged gas diffusivities at the experimental conditions. Also listed in the table are the previously reported[3,8] constant diffusivities, which—although for different LDPEs under different operating conditions—have values of the order 10^{-9} m^2 s^{-1} and exhibit the temperature and pressure effects discussed earlier. In particular, the rise in temperature is found to increase the diffusivity.

Sensitivity analysis

A sensitivity analysis was carried out to determine the effect of the deviation in the gas saturation mass concentration on diffusivity. Figure 6 compares actual gas diffusivity at 120°C and 1.31 MPa to those corresponding to ±2% variations in the gas phase volume. These variations conservatively embody the maximum possible error in the saturation gas mass concentration in the polymer, which is directly related to the gas phase volume. As observed from the figure, the three graphs overlap. In fact, the average of the absolute changes in the diffusivity is less than 0.007%.

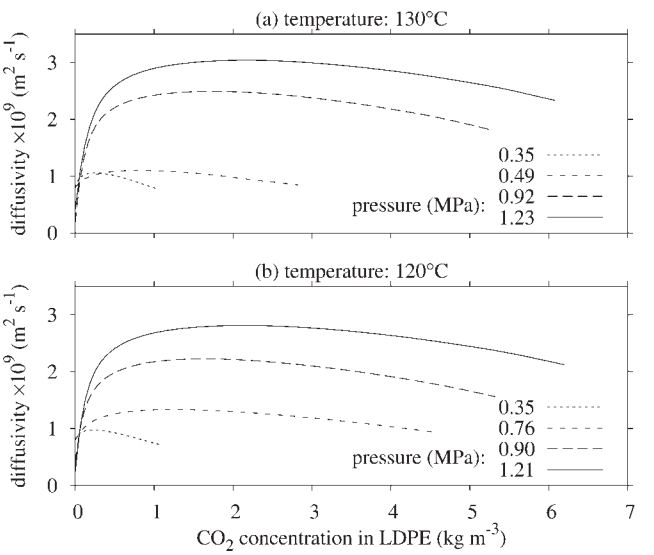

Figure 5 Diffusivity of carbon dioxide as a function of its mass fraction in the LDPE at different temperatures and pressures.

TABLE II
The Concentration-Averaged Diffusivity ($\times 10^9 m^2\ s^{-1}$) of CO_2 in LDPE Determined in this Work at Different Temperatures and Pressures

	LDPE characteristics			Temperature (°C)			
Reference	$M_n \times 10^{-3}$	$M_w \times 10^{-3}$	Pressure (MPa)	120	130	150	200
This work	12.1	89.056	0.35	0.88	0.95	–	–
			0.49	–	1.01	–	–
8	–	250	0.66	–	–	4.4	–
This work	12.1	89.056	0.76	1.20	–	–	–
			0.90	1.99	–	–	–
			0.92	–	2.25	–	–
			1.21	2.56	–	–	–
			1.23	–	2.78	–	–
8	–	250	1.57	–	–	3.9	–
			3.00	–	–	4.6	–
			3.37	–	–	4.4	–
3	15.2	105.5	12	–	–	–	9.92

Diffusivity values ($\times 10^9 m^2\ s^{-1}$) from previous investigations are also listed.

Mathematical correlations for diffusivity

The diffusivity versus gas mass concentration data obtained in this work were mathematically correlated to obtain the diffusivity as a function of gas mass concentration and pressure at a given temperature. Table Curve 3d™ was utilized to fit diffusivity, at a given temperature, as a simple polynomial function of pressure (P) and gas mass concentration (ω) with as few parameters as possible with an acceptable goodness of fit. With that criterion, the best function was found to be

$$D(P,\omega) = a_0 + a_1P + a_2P^2 + a_3P^3 + a_4\omega + a_5\omega^2 \quad (17)$$

In the above equation, D is in $m^2\ s^{-1}$, P is in MPa, and ω is in kg m^{-3}. Although the quadratic polynomial of ω suffices to describe the unimodal behavior of $D(\omega)$, the cubic polynomial of P is needed at the least to predict the multimodal $D(P)$. Table III lists the fitting parameters and details for eq. (17) at 120 and 130°C. At different temperature and pressure conditions, Figure 7 compares the absorbed gas mass calculated using eq. (17) to the experimental counterpart. Both masses agree very well except close to the peak temperature and pressure. The agreement could be improved but at the cost of more parameters and greater complexity in the equation to fit the diffusivity data. Equation (17), given its simplicity, manages well to predict the diffusivity.

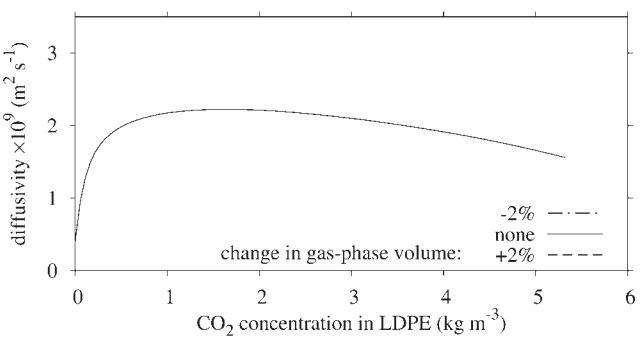

Figure 6 The effect of ±2% change in the gas-phase volume on $D(\omega)$ at 120°C and 1.31 MPa. (The three graphs overlap.)

CONCLUSIONS

A methodology was developed to experimentally determine the concentration-dependent diffusivity of a gas in a nonvolatile phase such as polymer. Based on pressure-decay experimentation, its detailed mass transfer model, and the calculus of variations, the diffusivity of carbon dioxide was determined as a function of its concentration in LDPE. The results were obtained at 120 and 130°C for four different pressures in the range 0.352 to 1.232 MPa. Generally of the order 10^{-9} $m^2\ s^{-1}$, the diffusivities were found to be strongly unimodal functions of gas concentration. The diffusivity at a given pressure increased with temperature, but showed a multimodal trend with pressure change at a given temperature. The sensitivity analyses carried out with respect to the

TABLE III
Parameters for the Diffusivity Correlation, eq. (17)

Parameter	120°C	130°C
a_0	7.67×10^{-9}	3.79×10^{-9}
a_1	-3.46×10^{-8}	-1.57×10^{-8}
a_2	4.93×10^{-8}	2.40×10^{-8}
a_3	-2.01×10^{-8}	-9.81×10^{-9}
a_4	2.84×10^{-10}	2.84×10^{-10}
a_5	-5.79×10^{-11}	-5.70×10^{-11}
r^2 coefficient	0.92	0.93
Fit std. error	2.03×10^{-10}	2.03×10^{-10}

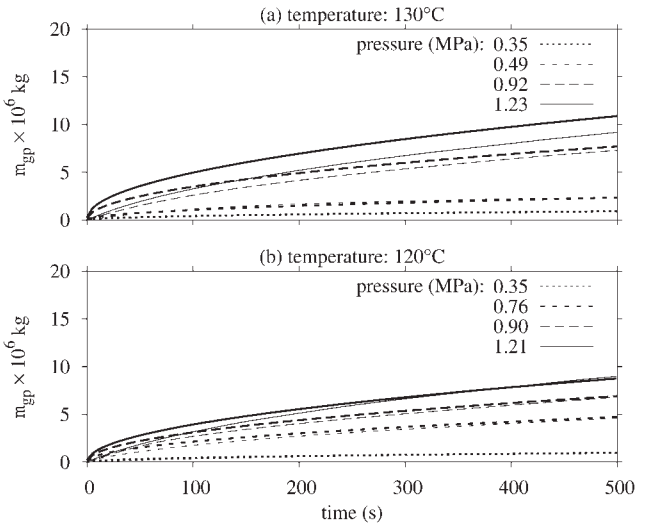

Figure 7 Comparison of eq. (17)-predicted gas mass absorbed (thicker line) with the experimental gas mass absorbed at different temperature and pressure conditions.

experimentally determined gas solubility and polymer density affirmed the reliability of the diffusivity results. Using a simple polynomial, the diffusivity was finally correlated with pressure and gas mass concentration at each experimental temperature.

NOMENCLATURE

a_i	parameters of eq. (17); ($i = 0, 1,\ldots,5$)
A	cross-sectional area of the polymer layer, m^2
d	internal diameter of the pressure vessel, m
D	diffusivity of gas in polymer, $m^2\ s^{-1}$
I	objective functional
J	variational derivative
K	augmented objective functional
L	thickness of the polymer sample, m
$m_{gp,m}$	calculated mass of gas absorbed in the polymer layer, kg
$m_{gp,e}$	experimental mass of gas absorbed in the polymer layer, kg
M_g	molar mass of gas, kg $kmol^{-1}$
M_n	number-average molecular weight of polymer, kg $kmol^{-1}$
M_w	weight-average molecular weight of polymer, kg $kmol^{-1}$
P	pressure, MPa
T	total experimental run time, s
V_{gp}	volume of gas–polymer mixture, m^3
V_p	volume of pure polymer, m^3
w	mass fraction of gas in the polymer layer
z	depth in the polymer layer, m
ρ_p	density of pure polymer, kg m^{-3}
λ	adjoint variable
ω	gas mass concentration in the polymer layer, kg m^{-3}
ω_{sat}	saturated ω, kg m^{-3}

We like to acknowledge the following: Dr. R. A. Heidemann, University of Calgary; Dr. S. Drappel, Xerox Research Center of Canada; Dr. J. Teh, Nova Chemicals; Dr. J. Soares, University of Waterloo.

APPENDIX

The optimal control problem is to find the find the function $D(\omega)$ that minimizes the following objective functional:

$$I = \int_0^T (m_{gp,m} - m_{gp,e})^2 dt = \int_0^T \left[\int_0^L \omega A dz - m_{gp,e}\right]^2 dt \tag{A1}$$

subject to the continuity equation, eq. (6), i.e.,

$$G = \frac{\partial \omega}{\partial t} - f = 0 \tag{A2}$$

where

$$f = D\left[1 + \frac{\omega}{\rho_p}\right]\frac{\partial^2 \omega}{\partial z^2} + \left[\left(1 + \frac{\omega}{\rho_p}\right)\frac{\partial D}{\partial \omega} + \frac{D}{\partial_p}\right]\left(\frac{\partial \omega}{\partial z}\right)^2 \tag{A3}$$

The above problem is equivalent to the unconstrained minimization of

$$K = I + \int_0^T \int_0^L [\lambda(z,t)G(z,t)]dzdt \tag{A4}$$

with $\lambda(z, t)$ as an adjoint variable.[16]

Necessary Condition for the Minimum

The necessary condition for the minimum is that the variation in K is zero[17], i.e.,

$$\delta K = \delta I + \int_0^T \int_0^L [\lambda(z,t)\delta G(z,t)]dzdt = 0 \tag{A5}$$

In the above equation,

$$\begin{aligned}\delta I &= \int_0^T 2(m_{gp,m} - m_{gp,e}) \int_0^L A\delta\omega dzdt \\ &= \int_0^T \int_0^L 2(m_{gp,m} - m_{gp,e})A\delta\omega dzdt\end{aligned} \tag{A6}$$

and δG is given by

$$\delta G = \frac{\partial}{\partial t}(\delta\omega) - \frac{\partial f}{\partial \omega}\delta\omega - \frac{\partial f}{\partial \omega_z}\delta\omega_z - \frac{\partial f}{\partial \omega_{zz}}\delta\omega_{zz} - \frac{\partial f}{\partial D}\delta D \tag{A7}$$

Substituting eqs. (A7) and (A6) into (A5) yields

$$\begin{aligned}\delta K = \int_0^T \int_0^L \Bigg[\left\{2(m_{gp,m} - m_{gp,e})A dzdt - \lambda\frac{\partial f}{\partial \omega}\right\}\delta\omega \\ + \lambda\left\{\frac{\partial(\delta\omega)}{\partial t} - \frac{\partial f}{\partial \omega_z}\delta\omega_z - \frac{\partial f}{\partial \omega_{zz}}\delta\omega_{zz} - \frac{\partial f}{\partial D}\delta D\right\}\Bigg] dzdt = 0\end{aligned} \tag{A8}$$

Integration by parts of the third, fourth, and fifth terms of the above equation yields

$$\int_0^T \int_0^L \lambda \frac{\partial(\delta\omega)}{\partial t} dz dt = \int_0^L \left\{ [\lambda \delta\omega]_0^T - \int_0^T \frac{\partial \lambda}{\partial t} \delta\omega dt \right\} dz \tag{A9}$$

$$\int_0^T \int_0^L \lambda \frac{\partial f}{\partial \omega_z} \delta\omega_z dz dt = \int_0^T \left\{ \left[\lambda \frac{\partial f}{\partial \omega_z} \delta\omega \right]_0^L - \int_0^L \frac{\partial}{\partial z} \left(\lambda \frac{\partial f}{\partial \omega_z} \right) \delta\omega dz \right\} dt \tag{A10}$$

$$\int_0^T \int_0^L \lambda \frac{\partial f}{\partial \omega_{zz}} \delta\omega_{zz} dz dt = \int_0^T \left\{ \left[\lambda \frac{\partial f}{\partial \omega_{zz}} \frac{\partial(\delta\omega)}{\partial z} - \frac{\partial}{\partial z} \left(\lambda \frac{\partial f}{\partial \omega_{zz}} \right) \delta\omega \right]_0^L + \int_0^L \frac{\partial^2}{\partial z^2} \left(\lambda \frac{\partial f}{\partial \omega_{zz}} \right) \delta\omega dz \right\} dt \tag{A11}$$

Substitution of eq. (A9)–(A11) into eq. (A8) gives

$$\begin{aligned} \delta K = & \int_0^T \int_0^L \left\{ -\frac{\partial \lambda}{\partial t} + 2(m_{\mathrm{gp},m} - m_{\mathrm{gp},e})A \right. \\ & \left. -\lambda \frac{\partial f}{\partial \omega} + \frac{\partial}{\partial z} \left(\lambda \frac{\partial f}{\partial \omega_z} \right) - \frac{\partial^2}{\partial z^2} \left(\lambda \frac{\partial f}{\partial \omega_{zz}} \right) \right\} \delta\omega dz dt \\ & - \int_0^T \int_0^L \lambda \frac{\partial f}{\partial D} \delta D dz dt + \int_0^L [\lambda \delta\omega]_0^T dz \\ & + \int_0^T \left[\lambda \frac{\partial f}{\partial \omega_z} - \frac{\partial}{\partial z} \left(\lambda \frac{\partial f}{\partial \omega_{zz}} \right) \right]_{z=0} \delta\omega(0,t) dt \\ & - \int_0^T \left[\lambda \frac{\partial f}{\partial \omega_z} - \frac{\partial}{\partial z} \left(\lambda \frac{\partial f}{\partial \omega_{zz}} \right) \right]_{z=L} \delta\omega(L,t) dt \\ & - \int_0^T \left[\lambda \frac{\partial f}{\partial \omega_{zz}} \frac{\partial(\partial\omega)}{\partial z} \right]_0^L dt = 0 \end{aligned} \tag{A12}$$

In the above equation, the first integral is eliminated by defining λ as

$$\frac{\partial \lambda}{\partial t} = 2(m_{\mathrm{gp},m} - m_{\mathrm{gp},e})A - \lambda \frac{\partial f}{\partial \omega} + \frac{\partial}{\partial z} \left(\lambda \frac{\partial f}{\partial \omega_z} \right) - \frac{\partial^2}{\partial z^2} \left(\lambda \frac{\partial f}{\partial \omega_{zz}} \right) \tag{A13}$$

The above equation has the following final form:

$$\frac{\partial \lambda}{\partial t} = 2A(m_{\mathrm{gp,mod}} - m_{\mathrm{gp},e}) + \frac{\lambda}{\rho_p} \frac{\partial D}{\partial \omega} \left(\frac{\partial \omega}{\partial z} \right)^2 + \left(1 + \frac{\omega}{\rho_p} \right) \left[\lambda \frac{\partial D}{\partial \omega} \frac{\partial^2 \omega}{\partial z^2} + \lambda \frac{\partial^2 D}{\partial \omega^2} \left(\frac{\partial \omega}{\partial z} \right)^2 - D \frac{\partial^2 \lambda}{\partial z^2} \right] \tag{13}$$

Because the initial mass concentration of the gas in the polymer is known at the interface and is zero elsewhere, the variation $\delta\omega(z, 0)$ is zero for all z. Since the final gas mass concentration is not specified, the third integral in eq. (A12) is eliminated by forcing

$$\lambda(z, T) = 0; \quad 0 \le z \le L \tag{14}$$

Since the equilibrium concentration of gas at the interface [$\omega(0,t) = \omega_{\mathrm{sat}}(t)$] is always specified, $\delta\omega(0,t)$ is zero. Thus, the fourth integral is eliminated in eq. (A12). Furthermore, by forcing

$$\lambda(L, t) = 0; \quad 0 \le t \le T \tag{15}$$

the fifth integral in eq. (A12) is eliminated. In addition to eq. (15), setting

$$\lambda(0, t) = 0; \ 0 \le t \le T \tag{16}$$

eliminates the sixth integral in eq. (A12). Note that eq. (14) is the final condition for eq. (13), which has eqs. (15) and (16) as its two boundary conditions.

Hence, subject to eqs. (13)–(16), eq. (A12) gets simplified to

$$\delta K = -\int_0^T \int_0^L \lambda \frac{\partial f}{\partial D} \delta D dz dt = 0 \tag{A14}$$

Thus, at the minimum of K, the variational derivative of K with respect to D is zero, i.e.,

$$J = -\lambda \frac{\partial f}{\partial D} = 0; \ 0 \le z \le L, \quad 0 \le t \le T \tag{12}$$

The negative of J provides the gradient correction for $D(\omega)$ in the iterative minimization of K.

References

1. Hirschfelder, J. O.; Curtiss, C. F.; Bird, R. B. Molecular Theory of Gases and Liquids; Wiley: New York, 1964.
2. Krishna, R.; Wesselingh, J. A. Chem Eng Sci 1997, 52, 861.
3. Areerat, S.; Funami, E.; Hayata, Y.; Nakagawa, D.; Ohshima, M. Polym Eng Sci 2004, 44, 1915.
4. Marais, S.; Hirata, Y.; Langevin, D.; Chappey, C. Mater Res Innov 2002, 6, 79.
5. Marais, S.; Saiter, J. M.; Devallencourt, C.; Nguyen, Q. T.; Métayer, M. Polym Test 2002, 21, 425.
6. Compan, V.; Ribes, A.; Diaz-Calleja, R.; Riande, E. Polymer 1996, 37, 2243.
7. Newitt, D. M.; Weale, K. E. J Chem Soc (London) 1948, IX, 1541.
8. Davis, P. K.; Lundy, G. D.; Palamara, J. E.; Duda, J. L.; Danner, R. P. Ind Eng Chem Res 2004, 43, 1537.
9. Lundenberg, J. L.; Wilk, M. B.; Huyett, M. J. Ind Eng Chem Fundam 1963, 2, 37.
10. Crank, J.; Park, G. S., eds. Diffusion in Polymers; Academic Press: New York, 1968; p 20.
11. Koros, W. J.; Paul, D. R.; Rocha, A. A. J Polym Sci B: Polym Phys 1976, 14, 687.
12. Koros, W. J.; Paul, D. R. J Polym Sci B: Polym Phys 1976, 14, 1903.
13. Upreti, S. R.; Mehrotra, A. K. Ind Eng Chem Res 2000, 39, 1080.
14. Vargaftik, N. B. Handbook of Physical Properties of Liquids and Gases: Pure Substances and Mixtures; Hemisphere: New York, 1980.
15. Press, W. H.; Teukolsky, S. A.; Vetterling, W. T.; Flannery, B. P. Numerical Recipes in C++, 2nd ed.; Cambridge University Press: New York, 2002.
16. Kirk, D. E. Optimal Control Theory; Dover Publications: New York, 2004; p 169.
17. Gelfand, I. M.; Fomin, S. V. Calculus of Variations; Dover Publications: New York, 2000; p 13.